
Random Projections with Asymmetric Quantization

Xiaoyun Li

Department of Statistics
Rutgers University
Piscataway, NJ 08854, USA
xiaoyun.li@rutgers.edu

Ping Li

Cognitive Computing Lab
Baidu Research
Bellevue, WA 98004, USA
liping11@baidu.com

Abstract

The method of random projection has been a popular tool for data compression, similarity search, and machine learning. In many practical scenarios, applying quantization on randomly projected data could be very helpful to further reduce storage cost and facilitate more efficient retrievals, while only suffering from little loss in accuracy. In real-world applications, however, data collected from different sources may be quantized under different schemes, which calls for a need to study the asymmetric quantization problem. In this paper, we investigate the cosine similarity estimators derived in such setting under the Lloyd-Max (LM) quantization scheme. We thoroughly analyze the biases and variances of a series of estimators including the basic simple estimators, their normalized versions, and their debiased versions. Furthermore, by studying the monotonicity, we show that the expectation of proposed estimators increases with the true cosine similarity, on a broader family of stair-shaped quantizers. Experiments on nearest neighbor search justify the theory and illustrate the effectiveness of our proposed estimators.

1 Introduction

The method of random projections (RP) [35] has become a popular technique to reduce data dimensionality while preserving distances between data points, as guaranteed by the celebrated Johnson-Lindenstrauss (J-L) Lemma and variants [24, 12, 1]. Given a high dimensional dataset, the algorithm projects each data point onto a lower-dimensional random subspace. There is a very rich literature of research on the theory and applications of random projections, such as clustering, classification, near neighbor search, bio-informatics, compressed sensing, etc. [22, 10, 4, 6, 8, 17, 18, 28, 15, 7, 19, 11, 9].

In recent years, “random projections + quantization” has been an active research topic. That is, the projected data, which are in general real-valued (i.e., infinite precision), are quantized into integers in a small number of bits. Applying quantization on top of random projections has at least two major advantages: (i) the storage cost is further (substantially) reduced; and (ii) some important applications such as hashing-table-based near neighbor search, require using quantized data for indexing purposes.

The pioneering example of quantized random projections should be the so-called “1-bit” (sign) random projections, initially used for analyzing the MaxCut problem [20] and then was adopted for near neighbor search [8] and compressed sensing [5, 23, 25]. As one would expect, storing merely 1-bit per projected data value in many situations might suffer from a substantial loss of accuracy, compared to using random projections with full (infinite) precision. There have been various studies on (symmetrically) quantized random projections beyond the 1-bit scheme, e.g., [13, 37, 26, 29, 31]. In this paper, we further move to studying “asymmetric quantization” of random projections, a relatively new problem arising from practical scenarios which is also mathematically very interesting.

Everyday, the process of data collection is taking place in every possible place that one can think of, but it is often impractical to cast a universal encoding strategy on data storage methods for every place. As a consequence, it becomes a meaningful task to look into the estimation problems with data encoded by different algorithms, or namely, the asymmetric case. In this paper, we provide

some insights on this type of problems, and particularly, we consider recovering inner products from asymmetrically quantized random projections, arising from the following two practical scenarios.

- **Scenario 1: quantization vs. full-precision.** Consider, for example, a retrieval system which uses random projections to process every data vector. To save storage, the projected data stored in the repository are quantized into a small number of bits. When a query data vector arrives, it is first processed by random projections. We then have the option of quantizing the projected query data vector before conducting the similarity search (with vectors in the repository); but we do not have to do the quantization step since we still have the projected query data vector in full-precision (why waste?). This situation hence creates the “quantization vs. full-precision” estimation problem. This setting is natural and practical, and the estimation problem has been studied in the literature, for example [14, 21, 27].
- **Scenario 2: quantization with different bits.** In applications such as large ad hoc networks [36, 30], data are collected and processed by different nodes (e.g., sensors or mobile devices) at different locations before sent to the central unit or cloud server. However, distinct nodes may use different quantization methods (or different bits) due to many possible reasons, e.g., memory capacity or purpose of data usage. In this situation, information retrieval among data sources using different quantization schemes could be on the cards. As a tightly related topic, asymmetric distributed source coding (with different bits from different sources) has also been considered in [3, 34] among others for sensor networks.

Scenario 1 is in fact an important special case of Scenario 2, where one source of data is quantized with infinite bits. In this paper, we provide thorough statistical analysis on the above two scenarios.

Our contributions. The major contributions of this paper include the following:

- In Section 3, we provide the bias and variance of linear and normalized inner product estimators in Scenario 1. We reveal an interesting connection between the variance of debiased inner product estimator and similarity search, which is very helpful in practice.
- In Sections 4 and 5, we conduct statistical analysis in Scenario 2, and prove the monotonicity of a large family of asymmetric quantized inner product estimators, which assures their validity for practical use. A new bound on the bias is also derived in the symmetric case.
- In Section 6, an empirical study on various real-world datasets confirms the theoretical findings and well illustrates the effectiveness of proposed quantized estimators.

2 Preliminaries

Random Projections. Let $U = [u_1, \dots, u_n]^T \in \mathbb{R}^{n \times d}$ be the original data matrix (with d possibly being large). Random projections are realized by $Z = [z_1, \dots, z_n]^T = U \times R$, where $R \in \mathbb{R}^{d \times k}$, $k \ll d$ is a random matrix with i.i.d. standard Gaussian entries. Let $\|\cdot\|_2$ denote the l_2 Euclidean norm. Throughout this paper, we assume that every data point is normalized to unit norm¹, i.e., $\|u_i\|_2 = 1$, $1 \leq i \leq n$. We will hence use the terms “inner product” and “cosine similarity” interchangeably.

For the convenience of presentation, our results (estimators and properties) will be given for two pairs of data vectors, u_i and u_j (and correspondingly z_i and z_j). Let $\rho = \langle u_i, u_j \rangle$ be the inner product between u_i and u_j . We also denote $x = z_i$ and $y = z_j$. It is then easy to verify that (x, y) is bi-variate normal:

$$\begin{pmatrix} x \\ y \end{pmatrix} \sim N \left(\begin{pmatrix} 0 \\ 0 \end{pmatrix}, \begin{pmatrix} 1 & \rho \\ \rho & 1 \end{pmatrix} \right). \quad (1)$$

Lloyd-Max (LM) quantization [33, 32]. Assume a random signal model with signals generated from a probability distribution with density $X \sim f$. An M -level scalar quantizer $q_M(\cdot)$ is specified by $M + 1$ decision borders $t_0 < t_1 < \dots < t_M$ and M reconstruction levels (or codes) μ_i , $i = 1, \dots, M$, with the quantizing operator defined as

$$q_M(x) = \mu_{i^*}, \quad i^* = \{i : t_{i-1} < x \leq t_i, 1 \leq i \leq M\}. \quad (2)$$

¹Normalizing each data vector to the unit norm is a standard data preprocessing procedure for many applications such as clustering and classification. In this paper, we adopt this assumption merely for convenience. When data is not normalized, our results still hold, although we will need to store the values of the norms.

The ‘‘distortion’’ is an important quantity that measures how much information is lost from the original signal due to quantization. In this paper, we will also assume $M = 2^b$, with $b = 1, 2, \dots$, being the number of bits used for the quantizer. Thus, we will write $q_b(\cdot)$ instead of $q_M(\cdot)$.

Definition 1. *The distortion of a b -bit quantizer $Q_b(\cdot)$ with respect to distribution f is defined as*

$$\mathbb{E}((X - q_b(X))^2) = \int (x - q_b(x))^2 f(x) dx = \sum_{i=1}^{2^b} \int_{t_{i-1}}^{t_i} (x - \mu_i)^2 f(x) dx. \quad (3)$$

In this paper, f is the standard normal, i.e., $f(x) = \phi(x) = \frac{1}{\sqrt{2\pi}} e^{-x^2/2}$ in the conventional notation for Gaussian. Also, we will use Q_b to denote Lloyd-Max (LM) quantizer which minimizes the distortion and D_b to denote the corresponding value of distortion:

$$Q_b = \underset{q}{\operatorname{argmin}} \mathbb{E}((X - q_b(X))^2), \quad D_b = \mathbb{E}((X - Q_b(X))^2) \quad (4)$$

A basic identity of LM quantizer is that $\mathbb{E}(Q_b^2(X)) = \mathbb{E}(Q_b(X)X)$. In practice, Lloyd’s algorithm [32] is used to find the solution, which alternates between updating borders and reconstruction points until convergence (and the convergence is guaranteed).

Estimates using full-precision RP’s. Consider observations $\begin{pmatrix} x_i \\ y_i \end{pmatrix} \stackrel{\text{i.i.d.}}{\sim} N\left(\begin{pmatrix} 0 \\ 0 \end{pmatrix}, \begin{pmatrix} 1 & \rho \\ \rho & 1 \end{pmatrix}\right)$, $1 \leq i \leq k$, as in (1). The task is to estimate ρ . One can use the usual simple estimator

$$\hat{\rho}_f = \frac{1}{k} \sum_{i=1}^k x_i y_i, \quad \text{with } \mathbb{E}(\hat{\rho}_f) = \rho, \quad \operatorname{Var}(\hat{\rho}_f) = \frac{1 + \rho^2}{k}. \quad (5)$$

where $\mathbb{E}(\hat{\rho})$ is the expectation and $\operatorname{Var}(\hat{\rho})$ is the variance. Note that the variance grows as $|\rho|$ increases. One can take advantage of the following so-called ‘‘normalized estimator’’:

$$\hat{\rho}_{f,n} = \frac{\sum_{i=1}^k x_i y_i}{\sqrt{\sum_{i=1}^k x_i^2} \sqrt{\sum_{i=1}^k y_i^2}}, \quad \mathbb{E}(\hat{\rho}_{f,n}) = \rho + O\left(\frac{1}{k}\right), \quad \operatorname{Var}(\hat{\rho}_{f,n}) = \frac{(1 - \rho^2)^2}{k} + O\left(\frac{1}{k^2}\right). \quad (6)$$

$\hat{\rho}_{f,n}$ is nearly unbiased but it substantially reduces the variance especially near two extreme points $\rho = \pm 1$. We refer readers to the classical textbook [2] and recent papers [28, 27] for more details.

Estimates using symmetric LM quantized RP’s. [29] study the inner product estimator under LM quantization scheme, by analyzing the biases and variances of estimators in the symmetric case. That is, the observations x_i and y_i are quantized by the same LM scheme with the same number of bits (b). In this paper, we study the asymmetric setting by using b_1 number of bits for quantizing x_i and b_2 number of bits for y_i . Apparently, the work of [29] is a special case of our results (i.e., $b_1 = b_2$). Interestingly, our analysis also leads to a more refined bound on the estimation bias in the symmetric case compared to the corresponding bound in [29]. See Section 4 for the detailed results.

3 Scenario 1: Quantization vs. Full-precision

Recall that, we have i.i.d. observations $\{x_i, y_i\}$, $i = 1, 2, \dots, k$, from a standard bi-variate normal with $x_i \sim N(0, 1)$, $y_i \sim N(0, 1)$, and $\mathbb{E}(x_i y_i) = \rho$. In this section, we study Scenario 1: quantization vs. full-precision. That is, we quantize x_i with b bits and we leave y_i intact. The task is to estimate ρ from $\{Q_b(x_i), y_i\}$, $i = 1, 2, \dots, k$. We can still try to use the simple estimator similar to (5):

$$\hat{\rho}_{b,f} = \frac{1}{k} \sum_{i=1}^k Q_b(x_i) y_i. \quad (7)$$

As one would expect, this estimator $\hat{\rho}_{b,f}$ is no longer unbiased. We can show that $\mathbb{E}(\hat{\rho}_{b,f}) = \xi_{1,1} \rho$. Hence, we can attempt to remove the bias by using the following ‘‘debiased estimator’’

$$\hat{\rho}_{b,f}^{db} = \frac{\hat{\rho}_{b,f}}{\xi_{1,1}} = \frac{1}{k} \frac{1}{\xi_{1,1}} \sum_{i=1}^k Q_b(x_i) y_i. \quad (8)$$

We will need to define $\xi_{1,1}$. More generally and analogous to the notation in [29], we define

$$\gamma_{\alpha,\beta} = \mathbb{E}(Q_b(x)^\alpha y^\beta), \quad \xi_{\alpha,\beta} = \mathbb{E}(Q_b(x)^\alpha x^\beta). \quad (9)$$

That is, $\xi_{1,1} = \mathbb{E}(Q_b(x)x)$. Note that $\xi_{\alpha,\beta}$ can be represented by $\gamma_{\alpha,\beta}$, but we use both for convenience. Also note that $\xi_{1,1} = \xi_{2,0} = 1 - D_b$ from definitions. For $b = 1, 2, 3, 4, \infty$, we can compute $\xi_{1,1} = 0.6366, 0.8825, 0.9655, 0.9905, 1$, respectively (keeping four decimal points). In fact, it is also known that $D_b = \frac{3^{3/2}2\pi}{12}2^{-2b}$, i.e., the bias decays at the rate of $O(2^{-2b})$. In the following, Theorem 1 summarizes the expectations and variances of the two estimators $\hat{\rho}_{b,f}$ and $\hat{\rho}_{b,f}^{db}$.

Theorem 1.

$$\mathbb{E}(\hat{\rho}_{b,f}) = \xi_{1,1}\rho, \quad \mathbb{E}(\hat{\rho}_{b,f}^{db}) = \rho, \quad (10)$$

$$\text{Var}(\hat{\rho}_{b,f}) = \frac{V_{b,f}}{k}, \quad \text{with } V_{b,f} = (\xi_{2,2} - \xi_{2,0} - \xi_{1,1}^2)\rho^2 + \xi_{2,0} \quad (11)$$

$$\text{Var}(\hat{\rho}_{b,f}^{db}) = \frac{V_{b,f}^{db}}{k}, \quad \text{with } V_{b,f}^{db} = \frac{(\xi_{2,2} - \xi_{2,0} - \xi_{1,1}^2)\rho^2 + \xi_{2,0}}{\xi_{1,1}^2}. \quad (12)$$

Normalized Estimator. We also attempt to take advantage of the (beneficial) effect of normalization by defining two normalized estimators and their variances, as summarized in Theorem 2.

Theorem 2. As $k \rightarrow \infty$, we have

$$\hat{\rho}_{b,f,n} = \frac{\sum_{i=1}^k Q_b(x_i)y_i}{\sqrt{\sum_{i=1}^k Q_b^2(x_i)}\sqrt{\sum_{i=1}^k y_i^2}}, \quad \mathbb{E}(\hat{\rho}_{b,f,n}) = \sqrt{\xi_{1,1}}\rho + O\left(\frac{1}{k}\right), \quad (13)$$

$$\hat{\rho}_{b,f,n}^{db} = \frac{\hat{\rho}_{b,f,n}}{\sqrt{\xi_{1,1}}}, \quad \mathbb{E}(\hat{\rho}_{b,f,n}^{db}) = \rho + O\left(\frac{1}{k}\right), \quad (14)$$

$$\text{Var}(\hat{\rho}_{b,f,n}) = \frac{V_{b,f,n}}{k} + O\left(\frac{1}{k^2}\right), \quad \text{Var}(\hat{\rho}_{b,f,n}^{db}) = \frac{V_{b,f,n}^{db}}{k} + O\left(\frac{1}{k^2}\right), \quad (15)$$

$$V_{b,f,n} = \left(\frac{\gamma_{4,0}}{4\gamma_{2,0}} + \frac{3}{4}\gamma_{2,0} + \frac{1}{2}\gamma_{2,2}\right)\rho^2 - \left(\frac{\gamma_{3,1}}{\gamma_{2,0}} + \gamma_{1,3}\right)\rho + \frac{\gamma_{2,2}}{\gamma_{2,0}}, \quad V_{b,f,n}^{db} = \frac{V_{b,f,n}}{\xi_{1,1}}. \quad (16)$$

3.1 Benefits of normalized estimators and debiased estimators

Figure 1 plots (in the left two panels) the variances for two debiased estimators $\hat{\rho}_{b,f}^{db}$ and $\hat{\rho}_{b,f,n}^{db}$, to illustrate the benefits of normalization. The right panel of Figure 1 demonstrates that the variance of the normalized estimator is always smaller, and substantially so as ρ away from zero.

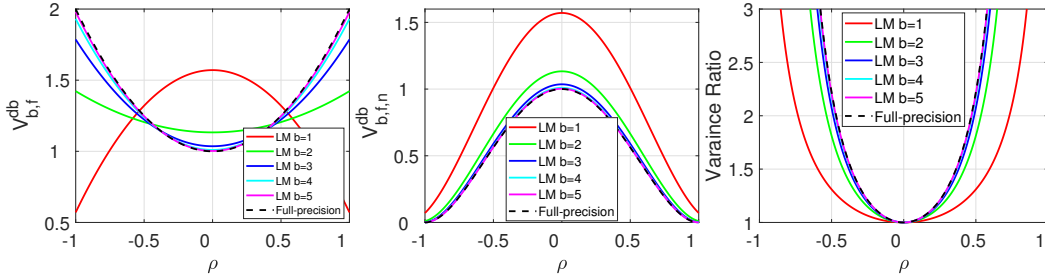


Figure 1: Scenario 1: Comparisons of theoretical variances between two (debiased) estimators $\hat{\rho}_{b,f}^{db}$ and $\hat{\rho}_{b,f,n}^{db}$. **Left panel:** the variance factor $V_{b,f}^{db}$ for $b = 1, 2, 3, 4, 5, \infty$. **Middle panel:** the variance factor $V_{b,f,n}^{db}$ (for the normalized estimator). **Right panel:** the variance ratio: $\frac{V_{b,f}^{db}}{V_{b,f,n}^{db}}$.

To elaborate on the benefit of debiased estimators, we evaluate the mean square errors (MSE): bias² + variance. Given the benefit of normalization, we consider the two normalized estimators:

$$\text{MSE}(\hat{\rho}_{b,f,n}) = \left(1 - \sqrt{\xi_{1,1}}\right)^2 \rho^2 + \frac{V_{b,f,n}}{k} + O\left(\frac{1}{k^2}\right), \quad \text{MSE}(\hat{\rho}_{b,f,n}^{db}) = \frac{V_{b,f,n}^{db}}{\xi_{1,1}k} + O\left(\frac{1}{k^2}\right).$$

Thus, to compare their mean square errors, we can examine the ratio: $\xi_{1,1} + k\rho^2 \frac{\xi_{1,1}(1-\sqrt{\xi_{1,1}})^2}{V_{b,f,n}}$, which will be larger than 1 quickly as k increases. Note that $\xi_{1,1} \leq 1$ but it is very close to 1 when $b \geq 3$. In summary, the MSE of the debiased estimator quickly becomes smaller as k increases.

3.2 Analysis of mis-ordering probabilities in similarity search

In similarity search, the estimates of inner products are subsequently used for ordering data vectors to identify the nearest neighbor for a given query. Intuitively, a more accurate estimator should provide a more accurate ordering, but a precise analysis is needed for the “mis-ordering” probabilities.

Definition 2. Suppose $u_1, u_2, u_3 \in \mathbb{R}^d$ are three data points (with u_1 being a query) with unit norm and pair-wise cosine similarity ρ_{12}, ρ_{13} and ρ_{23} respectively. For an estimator $\hat{\rho}$, the probability of *mis-ordering* is defined as

$$P_{\mathcal{M}}(u_1; u_2, u_3) = Pr(\hat{\rho}_{12} > \hat{\rho}_{13} | \rho_{12} < \rho_{13}).$$

Consider a case where u_3 is the nearest point of u_1 in the data space (which implies $\rho_{12} < \rho_{13}$). If the estimation gives $\hat{\rho}_{12} > \hat{\rho}_{13}$, we then make a wrong decision that u_3 is not the nearest neighbor of u_1 .

Theorem 3. (Asymptotic mis-ordering) Suppose $u_1, u_2, u_3 \in \mathbb{R}^d$ are three data points (with u_1 being the query) on a unit sphere with pair-wise inner products ρ_{12}, ρ_{13} and ρ_{23} respectively. Denote two estimators $\hat{\rho}$ and $\hat{\rho}'$ based on k random projections such that as $k \rightarrow \infty$, the normality $\hat{\rho} \sim N(\alpha\rho, \hat{\sigma}_\rho^2)$ and $\hat{\rho}' \sim N(\alpha'\rho, \hat{\sigma}'_\rho{}^2)$ hold, with constants $\alpha, \alpha' > 0$. Denote $\delta_\rho^2 = \frac{\hat{\sigma}_\rho^2}{\alpha^2}$, $\delta'_\rho{}^2 = \frac{\hat{\sigma}'_\rho{}^2}{\alpha'^2}$ and the correlations $C = \text{corr}(\hat{\rho}_{12}, \hat{\rho}_{13})$, $C' = \text{corr}(\hat{\rho}'_{12}, \hat{\rho}'_{13})$, respectively. If

$$\delta'_{\rho_{12}} = a\delta_{\rho_{12}}, \quad \delta'_{\rho_{13}} = a'\delta_{\rho_{13}}, \quad C - aa'C' < \frac{(1-a^2)\delta_{\rho_{12}}^2 + (1-a'^2)\delta_{\rho_{13}}^2}{2\delta_{\rho_{12}}\delta_{\rho_{13}}}, \quad (17)$$

with some $0 < a < 1$, $0 < a' < 1$, then as $k \rightarrow \infty$ we have $\hat{P}_{\mathcal{M}}(u_1; u_2, u_3) > \hat{P}'_{\mathcal{M}}(u_1; u_2, u_3)$, where $\hat{P}_{\mathcal{M}}(u_1; u_2, u_3)$ and $\hat{P}'_{\mathcal{M}}(u_1; u_2, u_3)$ are the mis-ordering probability of $\hat{\rho}$ and $\hat{\rho}'$, respectively.

Remark. There is an interesting connection with the variances of the aforementioned “debiased estimators”. Condition (17) basically assumes that the variance of the debiased $\hat{\rho}'$ is smaller than that of the debiased $\hat{\rho}$ at ρ_{12} and ρ_{13} respectively by factors a and a' . In a special case where $a = a'$ and $C = C'$, the last constraint in (17) reduces to $C < \frac{\delta_{\rho_{12}}^2 + \delta_{\rho_{13}}^2}{2\delta_{\rho_{12}}\delta_{\rho_{13}}}$, which always holds since the right-hand side is greater than 1. Also, note that, by Central Limit Theorem, the normality assumption is true for all the estimators we have discussed in this paper.

Although Theorem 3 is asymptotic, we are able to obtain valuable insights in finite sample case, since statistically a sufficiently large k is enough to provide good approximation to the normal distribution. The important message given by Theorem 3 is that estimators with lower “debiased variance” (δ) tend to have lower mis-ordering probability, which leads to a more accurate estimation of nearest neighbors in the original data space. This could be extremely feasible in numerous real world applications.

4 Scenario 2: Quantization with Different Bits

We now consider the more general case (Scenario 2) where the data vectors are LM quantized with different numbers of bits. That is, given observations $\{x_i, y_i\}$, $1 \leq i \leq n$, we quantize x_i using b_1 bits and y_i using b_2 bits. Without loss of generality, we assume $b_1 < b_2$. Furthermore, we denote two Lloyd-Max quantizers as Q_{b_1} and Q_{b_2} and distortion D_{b_1} and D_{b_2} , respectively. Similar to Scenario 1, we define the asymmetric estimator and the corresponding normalized estimator as

$$\hat{\rho}_{b_1, b_2} = \frac{1}{k} \sum_{i=1}^k Q_{b_1}(x_i) Q_{b_2}(y_i), \quad \hat{\rho}_{b_1, b_2, n} = \frac{\sum_{i=1}^k Q_{b_1}(x_i) Q_{b_2}(y_i)}{\sqrt{\sum_{i=1}^k Q_{b_1}^2(x_i)} \sqrt{\sum_{i=1}^k Q_{b_2}^2(y_i)}}. \quad (18)$$

As one might expect, the analysis will become somewhat more difficult. Similar to the analysis for Scenario 1, in this section we will use the following notations:

$$\xi_{\alpha, \beta} = \mathbb{E}(Q_{b_1}(x)^\alpha x^\beta), \quad \gamma_{\alpha, \beta} = \mathbb{E}(Q_{b_2}(x)^\alpha x^\beta), \quad \zeta_{\alpha, \beta} = \mathbb{E}(Q_{b_1}(x)^\alpha Q_{b_2}(y)^\beta), \quad (19)$$

which allow us to express the expectation and variance of $\hat{\rho}_{b_1, b_2}$ as follows.

$$\mathbb{E}(\hat{\rho}_{b_1, b_2}) = \zeta_{1,1}, \quad \text{Var}(\hat{\rho}_{b_1, b_2}) = \frac{V_{b_1, b_2}}{k}, \quad V_{b_1, b_2} = \zeta_{2,2} - \zeta_{1,1}^2 \quad (20)$$

$\zeta_{1,1}$ can be expressed as an infinite sum, but it appears difficult to be further simplified. Nevertheless, we are able to quantify the expectation of $\hat{\rho}_{b_1, b_2}$ in Theorem 4.

Theorem 4. *The following two bounds hold for $\rho \in [-1, 1]$:*

$$|\mathbb{E}(\hat{\rho}_{b_1, b_2}) - (1 - D_{b_1})(1 - D_{b_2})\rho| \leq \Delta_1, \quad \text{and} \quad (21)$$

$$\Delta_2 - \Delta_1 \leq |E(\hat{\rho}_{b_1, b_2}) - \rho| \leq \Delta_1 + \Delta_2, \quad \text{where} \quad (22)$$

$$\Delta_1 = \sqrt{D_{b_1} D_{b_2}} \sqrt{1 - D_{b_1}} \sqrt{1 - D_{b_2}} |\rho|^3, \quad \Delta_2 = (D_{b_1} + D_{b_2} - D_{b_1} D_{b_2}) |\rho|.$$

Remark. *When $b_2 \rightarrow \infty$ (i.e., Scenario 1), we have $D_{b_2} \rightarrow 0$ and the bound reduces to an equality $\mathbb{E}(\hat{\rho}_{b_1, \infty}) = (1 - D_{b_1})\rho$, which matches the result in Section 3.*

Eq. (22) provides upper and lower bounds for the absolute bias of $\hat{\rho}_{b_1, b_2}$. When $b_1 = b_2$ (i.e., the symmetric quantization case), Theorem 5 presents more refined bounds of the bias of $\hat{\rho}_{b_1, b_2}$.

Theorem 5. (Symmetric quantization) *Suppose $b_1 = b_2 = b$. For $\rho \in [-1, 1]$, we have*

$$(2D_b - D_b^2)|\rho| - D_b(1 - D_b)|\rho|^3 \leq |\mathbb{E}(\hat{\rho}_{b, b}) - \rho| \leq (2D_b - D_b^2)|\rho|. \quad (23)$$

Remark. *Compared to [29], which derived $|\mathbb{E}(\hat{\rho}_{b, b}) - \rho| \leq 2D_b|\rho|$, our bounds are more tight.*

What about the debiased estimator of $\hat{\rho}_{b_1, b_2}$? It is slightly tricky because $\mathbb{E}(\hat{\rho}_{b_1, b_2}) = \zeta_{1,1}$ cannot be explicitly expressed as $c\rho$ for some constant c (otherwise the debiased estimator would be simply $\hat{\rho}_{b_1, b_2}/c$). In Theorem 4, Eq. (21) implies that the expectation of $\hat{\rho}_{b_1, b_2}$ is close to $(1 - D_{b_1})(1 - D_{b_2})\rho$. Thus, we recommend $\frac{\hat{\rho}_{b_1, b_2}}{(1 - D_{b_1})(1 - D_{b_2})}$ as the surrogate for the debiased estimator.

Next, we provide the expectation and variance of the normalized estimator in Theorem 6.

Theorem 6. (Normalized estimator) *As $k \rightarrow \infty$, we have*

$$\mathbb{E}(\hat{\rho}_{b_1, b_2, n}) = \frac{\zeta_{1,1}}{\sqrt{\xi_{2,0}\gamma_{2,0}}} + O\left(\frac{1}{k}\right), \quad \text{Var}(\hat{\rho}_{b_1, b_2, n}) = \frac{V_{b_1, b_2, n}}{k} + O\left(\frac{1}{k^2}\right), \quad (24)$$

$$V_{b_1, b_2, n} = \frac{\zeta_{2,2} - \zeta_{1,1}^2}{\xi_{2,0}\gamma_{2,0}} - \frac{\zeta_{1,1}\zeta_{3,1} - \zeta_{1,1}^2\xi_{2,0}}{\xi_{2,0}^2\gamma_{2,0}} - \frac{\zeta_{1,1}\zeta_{1,3} - \zeta_{1,1}^2\gamma_{2,0}}{\xi_{2,0}\gamma_{2,0}^2} \quad (25)$$

$$+ \frac{\zeta_{1,1}^2\zeta_{2,2} - \zeta_{1,1}^2\xi_{2,0}\gamma_{2,0}}{2\xi_{2,0}^2\gamma_{2,0}^2} + \frac{\zeta_{1,1}^2\xi_{4,0} - \zeta_{1,1}^2\xi_{2,0}^2}{4\xi_{2,0}^3\gamma_{2,0}} + \frac{\zeta_{1,1}^2\gamma_{4,0} - \zeta_{1,1}^2\gamma_{2,0}^2}{4\xi_{2,0}\gamma_{2,0}^3}.$$

Remark. *When $b_2 = \infty$, the expected value of $\hat{\rho}_{b_1, b_2, n}$ reduces to that of $\hat{\rho}_{b_1, f, n}$ in Scenario 1. Additionally, we have $\zeta_{1,1} = \zeta_{2,0}\rho$, $\gamma_{2,0} = 1$, and $\gamma_{4,0} = 3$. It is easy to check that the expression of the variance will reduce to the corresponding formula in Theorem 2. Also, note that $\xi_{2,0} = 1 - D_{b_1}$, $\gamma_{2,0} = 1 - D_{b_2}$, and $\zeta_{1,1} \approx (1 - D_{b_1})(1 - D_{b_2})\rho$. This means that we can practically use $\frac{\hat{\rho}_{b_1, b_2, n}}{\sqrt{(1 - D_{b_1})(1 - D_{b_2})}}$ as surrogate for the debiased estimator of $\hat{\rho}_{b_1, b_2, n}$.*

We plot the related results in Figure 2, which verifies the theories in Theorems 4, 5 and 6.

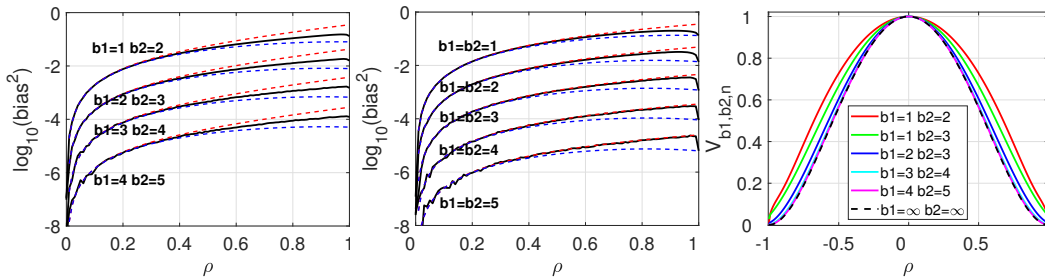


Figure 2: **Left panel:** the absolute bias (solid curves, in \log_{10} scale) of $\hat{\rho}_{b_1, b_2}$ by simulations, along with the upper bound (red dashed curves) and lower bound (blue dashed curves) in Eq. (22). **Middle panel:** the absolute bias of $\hat{\rho}_{b_1, b_2}$ with $b_1 = b_2$ (the symmetric case) along with the upper and lower bounds in Eq. (23). **Right panel:** The variance $V_{b_1, b_2, n}$ of the normalized estimator in Theorem 6.

5 Monotonicity of Inner Product Estimates

In applications such as nearest neighbor retrieval, the order of distances tends to matter more than the exact values. Given an estimator $\hat{\rho}$, one would hope that $\mathbb{E}(\hat{\rho})$ is monotone in ρ . This is indeed

the case in the full-precision situation. Recall that, in Section 2, given i.i.d. observations $\{x_i, y_i\}$, $i = 1, 2, \dots, k$, the full-precision estimator $\hat{\rho}_f = \frac{1}{k} \sum_{i=1}^k x_i y_i$ is monotone in ρ in the expectation because $\mathbb{E}(\hat{\rho}_f) = \rho$. Naturally, one will ask if the expectations of our quantized estimators, e.g., $\hat{\rho}_{b_1, b_2} = \frac{1}{k} \sum_{i=1}^k Q_{b_1}(x_i) Q_{b_2}(y_i)$, are also monotone in ρ . This turns out to be non-trivial question.

We solve this important problem rigorously through several stages. Our analysis will not be restricted to LM quantizers. To do so, we will need the following definition about ‘‘increasing quantizer’’.

Definition 3. (Increasing quantizer) Let Q be an M -level quantizer with boarders $t_0 < \dots < t_M$ and reconstruction levels μ_1, \dots, μ_M . We say that Q is an increasing quantizer if $\mu_1 < \dots < \mu_M$.

To proceed, we will prove the following three Lemmas for increasing quantizers.

Lemma 1. (1-bit vs. others) Suppose Q_{b_1}, Q_{b_2} are increasing quantizers symmetric about 0, with $b_1 \geq 1$, and $b_2 = 1$. Then $\mathbb{E}(Q_{b_1}(x)Q_{b_2}(y))$ is strictly increasing in ρ on $[-1, 1]$.

Lemma 2. (2-bit vs. 2-bit) Suppose Q_{b_1}, Q_{b_2} are any two increasing quantizers symmetric about 0, with $b_1 = b_2 = 2$. Then $\mathbb{E}(Q_{b_1}(x)Q_{b_2}(y))$ is strictly increasing in ρ on $[-1, 1]$.

Lemma 3. (Universal decomposition) For any increasing discrete quantizer Q_b , $b \geq 3$ which is symmetric about 0, there exist a 2-bit symmetric increasing quantizer Q_2 and a $(b-1)$ -bit symmetric increasing quantizer Q_{b-1} such that $Q_b = Q_{b-1} + Q_2$.

Once we have the above lemmas, we are ready to prove the monotonicity of $\mathbb{E}(Q_{b_1}(x)Q_{b_2}(y))$.

Theorem 7. (Monotonicity) For any increasing quantizers Q_{b_1} and Q_{b_2} symmetric about 0 with bits $b_1 \geq 1$ and $b_2 \geq 1$, the function $\mathbb{E}(Q_{b_1}(x)Q_{b_2}(y))$ is increasing in ρ .

Proof. By Lemma 1, we know that the statement is valid for $b_1 = 1$, and arbitrary b_2 . Now we look at the case where $b_1 \geq 2, b_2 \geq 2$. By Lemma 3, we can always write

$$Q_{b_1}(x) = \sum_{i=1}^{b_1-1} \tilde{Q}_2^{(i)}(x), \quad Q_{b_2}(y) = \sum_{j=1}^{b_2-1} \hat{Q}_2^{(j)}(y),$$

where $\tilde{Q}_2^1, \dots, \tilde{Q}_2^{b_1-1}$ and $\hat{Q}_2^1, \dots, \hat{Q}_2^{b_2-1}$ are two sets of symmetric increasing 2-bit quantizers. Thus,

$$\begin{aligned} \frac{\partial \mathbb{E}(Q_{b_1}(x)Q_{b_2}(y))}{\partial \rho} &= \frac{\partial \mathbb{E}(\sum_{i=1}^{b_1-1} \tilde{Q}_2^{(i)}(x) \sum_{j=1}^{b_2-1} \hat{Q}_2^{(j)}(y))}{\partial \rho} \\ &= \sum_{i=1}^{b_1-1} \sum_{j=1}^{b_2-1} \frac{\partial \mathbb{E}(\tilde{Q}_2^{(i)}(x)\hat{Q}_2^{(j)}(y))}{\partial \rho} > 0, \end{aligned}$$

where the last equality is due to linearity of expectation and derivative, and the inequality holds because of Lemma 2. Therefore, $\mathbb{E}(Q_{b_1}(x)Q_{b_2}(y))$ is increasing in ρ for any $b_1 \geq 1$ and $b_2 \geq 1$. \square

Recall that, in Section 3.2, we have proved the result for the mis-ordering probability, i.e., Theorem 3, which actually assumes estimators have expectations monotone in ρ . Therefore, Theorem 7 provides the necessary proof to support the assumption in Theorem 3.

6 Empirical Study: Similarity Search

In this section, we test proposed estimators on 3 datasets from the UCI repository (Table 1) [16]. The experiments clearly confirm that the normalization step uniformly improves the search accuracy. The results also, to an extent, illustrate the influence of mis-ordering probability studied in Theorem 3.

Table 1: Datasets used in the empirical study. Mean ρ is the average pair-wise cosine similarity for sample pairs. Mean 1-NN ρ is the average cosine similarity of each point to its nearest neighbor.

Dataset	# samples	# features	# classes	Mean ρ	Mean 1-NN ρ
Arcene	200	10000	2	0.63	0.86
BASEHOCK	1993	4862	2	0.33	0.59
COIL20	1440	1024	20	0.61	0.93

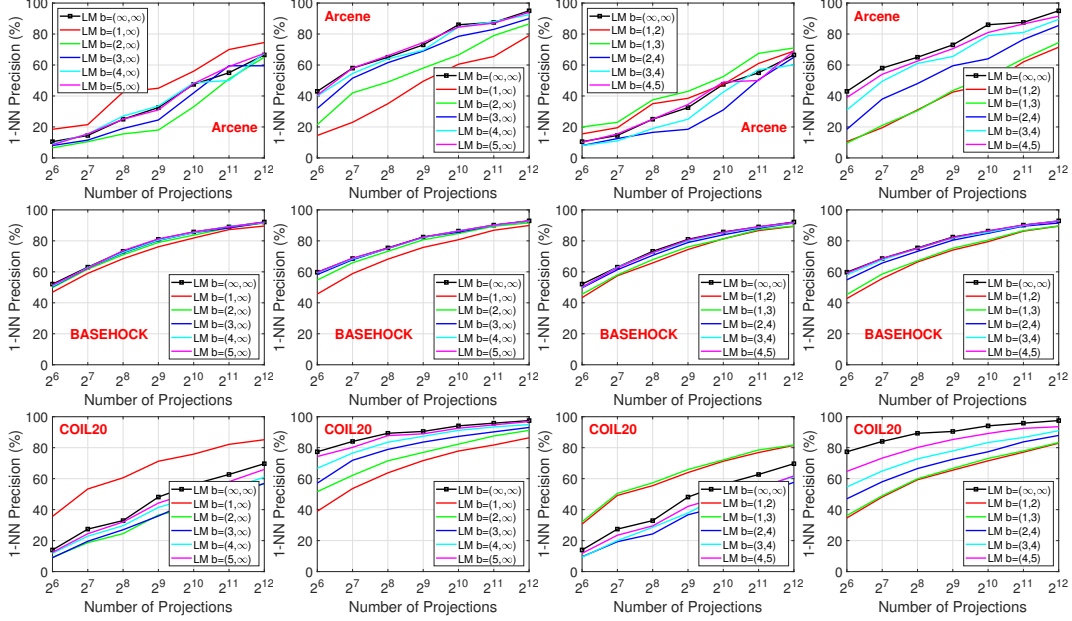


Figure 3: Nearest neighbor search recovery results using cosine similarity and quantized estimators, from random projections. Columns 1 and 2 (Scenario 1): the estimator $\hat{\rho}_{b,f}$ and its normalized version $\hat{\rho}_{b,f,n}$. Columns 3 and 4 (Scenario 2): the estimator $\hat{\rho}_{b_1,b_2}$ and its normalized version $\hat{\rho}_{b_1,b_2,n}$.

For each dataset, all the examples are preprocessed to have unit norm. The evaluation metric we adopt is the **1-NN precision**, which is the proportion of nearest neighbors (NN) we can recover from the nearest neighbor estimated using quantized random projections, averaged over all the examples.

We summarize the results in Figure 3. First of all, we can see that, as the number of bits increases, the performance of the quantized estimators converges to that of the estimator with full-precision, as expected. Importantly, the normalization step of the estimators substantially improves the performances, by comparing Column 2 with Column 1 (for Scenario 1), and Column 4 with Column 3 (for Scenario 2). In addition, we can to an extent validate the assertions in Theorem 3, which states that smaller variance of debiased estimators could improve NN recovery precision.

- In Figure 1 (left panel), we see that the variance of debiased estimate $\hat{\rho}_{b,f}^{db}$ with $b = 1$ is much smaller than using $b \geq 2$ in high similarity region (e.g. $|\rho| > 0.8$), and roughly the same at $\rho = 0.6$. Since *Arcene* and *COIL20* have high mean 1-NN ρ (0.86 and 0.93 respectively), Theorem 3 may imply that cosine estimation of $\hat{\rho}_{1,f}^{db}$ should (in general) have smaller mis-ordering probability than $b \geq 2$, implying higher 1-NN precision. On the other hand, the average 1-NN ρ of *BASEHOCK* is 0.59, so $\hat{\rho}_{b,f}^{db}$ with all $b = 1, 2, \dots, \infty$ would likely give similar performance. These claims are consistent with Column 1 of Figure 3.
- The variance of the debiased normalized estimator $\hat{\rho}_{b,f,n}^{db}$ (Figure 1, middle panel) decreases as b increases, uniformly for any ρ . Hence by Theorem 3 we expect the 1-NN precision should increase with larger b on all 3 datasets, as confirmed by Column 2 of Figure 3.

7 Conclusion

In this paper, we conduct a comprehensive study of estimating inner product similarities from random projections followed by asymmetric quantizations. This setting is theoretically interesting and also has many practical applications. For example, in a retrieval system, data vectors (after random projections) in the repository are quantized to reduce storage and communications; when a new query vector arrives, it does not have to be quantized. Another example of asymmetric quantization may come from data collected from different sources with own quantization strategies. In this study, we propose a series of estimators for asymmetric quantization, starting with the simple basic estimator, then the normalized estimator, and then the debiased estimators. We provide a thorough analysis of the estimation errors. Furthermore, we analyze the problems of “mis-ordering” probabilities and monotonicity properties of estimators. While our methods and analyses are largely based on the classical Lloyd-Max (LM) method, they can be extended to other more general quantization schemes.

References

- [1] Dimitris Achlioptas. Database-friendly random projections: Johnson-Lindenstrauss with binary coins. *Journal of Computer and System Sciences*, 66(4):671–687, 2003.
- [2] Theodore W. Anderson. *An Introduction to Multivariate Statistical Analysis*. John Wiley & Sons, third edition, 2003.
- [3] Jay M. Berger. A note on error detection codes for asymmetric channels. *Information and Control*, 4(1):68–73, 1961.
- [4] Ella Bingham and Heikki Mannila. Random projection in dimensionality reduction: Applications to image and text data. In *Proceedings of the Seventh ACM SIGKDD International Conference on Knowledge Discovery and Data Mining (KDD)*, pages 245–250, San Francisco, CA, 2001.
- [5] Petros Boufounos and Richard G. Baraniuk. 1-bit compressive sensing. In *42nd Annual Conference on Information Sciences and Systems (CISS)*, pages 16–21, Princeton, NJ, 2008.
- [6] Jeremy Buhler and Martin Tompa. Finding motifs using random projections. *Journal of Computational Biology*, 9(2):225–242, 2002.
- [7] Emmanuel Candès, Justin Romberg, and Terence Tao. Robust uncertainty principles: exact signal reconstruction from highly incomplete frequency information. *IEEE Transactions on Information Theory*, 52(2):489–509, Feb 2006.
- [8] Moses S. Charikar. Similarity estimation techniques from rounding algorithms. In *Proceedings on 34th Annual ACM Symposium on Theory of Computing (STOC)*, pages 380–388, Montreal, Canada, 2002.
- [9] George E. Dahl, Jack W. Stokes, Li Deng, and Dong Yu. Large-scale malware classification using random projections and neural networks. In *IEEE International Conference on Acoustics, Speech and Signal Processing (ICASSP)*, pages 3422–3426, Vancouver, Canada, 2013.
- [10] Sanjoy Dasgupta. Experiments with random projection. In *Proceedings of the 16th Conference in Uncertainty in Artificial Intelligence (UAI)*, pages 143–151, Stanford, CA, 2000.
- [11] Sanjoy Dasgupta and Yoav Freund. Random projection trees and low dimensional manifolds. In *Proceedings of the 40th Annual ACM Symposium on Theory of Computing (STOC)*, pages 537–546, Victoria, Canada, 2008.
- [12] Sanjoy Dasgupta and Anupam Gupta. An elementary proof of a theorem of Johnson and Lindenstrauss. *Random Structures and Algorithms*, 22(1):60 – 65, 2003.
- [13] Mayur Datar, Nicole Immorlica, Piotr Indyk, and Vahab S. Mirrokni. Locality-sensitive hashing scheme based on p-stable distributions. In *Proceedings of the 20th ACM Symposium on Computational Geometr (SCG)*, pages 253 – 262, Brooklyn, NY, 2004.
- [14] Wei Dong, Moses Charikar, and Kai Li. Asymmetric distance estimation with sketches for similarity search in high-dimensional spaces. In *Proceedings of the 31st Annual International ACM SIGIR Conference on Research and Development in Information Retrieval (SIGIR)*, pages 123–130, 2008.
- [15] David L. Donoho. Compressed sensing. *IEEE Transactions on Information Theory*, 52(4):1289–1306, April 2006.
- [16] Dheeru Dua and Casey Graff. UCI machine learning repository, 2017.
- [17] Ronald Fagin, Ravi Kumar, and D. Sivakumar. Efficient similarity search and classification via rank aggregation. In *Proceedings of the 2003 ACM SIGMOD International Conference on Management of Data (SIGMOD)*, pages 301–312, San Diego, CA, 2003.
- [18] Xiaoli Zhang Fern and Carla E. Brodley. Random projection for high dimensional data clustering: A cluster ensemble approach. In *Proceedings of the Twentieth International Conference (ICML)*, pages 186–193, Washington, DC, 2003.

- [19] Yoav Freund, Sanjoy Dasgupta, Mayank Kabra, and Nakul Verma. Learning the structure of manifolds using random projections. In *Advances in Neural Information Processing Systems (NIPS)*, pages 473–480, Vancouver, Canada, 2007.
- [20] Michel X. Goemans and David P. Williamson. Improved approximation algorithms for maximum cut and satisfiability problems using semidefinite programming. *Journal of ACM*, 42(6):1115–1145, 1995.
- [21] Albert Gordo, Florent Perronnin, Yunchao Gong, and Svetlana Lazebnik. Asymmetric distances for binary embeddings. *IEEE Trans. Pattern Anal. Mach. Intell.*, 36(1):33–47, 2014.
- [22] Piotr Indyk and Rajeev Motwani. Approximate nearest neighbors: Towards removing the curse of dimensionality. In *Proceedings of the Thirtieth Annual ACM Symposium on the Theory of Computing (STOC)*, pages 604–613, Dallas, TX, 1998.
- [23] Laurent Jacques, Jason N. Laska, Petros T. Boufounos, and Richard G. Baraniuk. Robust 1-bit compressive sensing via binary stable embeddings of sparse vectors. *IEEE Transactions on Information Theory*, 59(4):2082–2102, 2013.
- [24] William B. Johnson and Joram Lindenstrauss. Extensions of Lipschitz mapping into Hilbert space. *Contemporary Mathematics*, 26:189–206, 1984.
- [25] Ping Li. One scan 1-bit compressed sensing. In *Proceedings of the 19th International Conference on Artificial Intelligence and Statistics (AISTATS)*, pages 1515–1523, Cadiz, Spain, 2016.
- [26] Ping Li. Binary and multi-bit coding for stable random projections. In *Proceedings of the 20th International Conference on Artificial Intelligence and Statistics (AISTATS)*, pages 1430–1438, Fort Lauderdale, FL, 2017.
- [27] Ping Li. Sign-full random projections. In *The Thirty-Third AAAI Conference on Artificial Intelligence (AAAI)*, pages 4205–4212, Honolulu, Hawaii, 2019.
- [28] Ping Li, Trevor J. Hastie, and Kenneth W. Church. Improving random projections using marginal information. In *19th Annual Conference on Learning Theory (COLT)*, pages 635–649, Pittsburgh, PA, 2006.
- [29] Ping Li and Martin Slawski. Simple strategies for recovering inner products from coarsely quantized random projections. In *Advances in Neural Information Processing Systems (NIPS)*, pages 4567–4576, Long Beach, CA, 2017.
- [30] Xiang-Yang Li. *Wireless ad hoc and sensor networks: theory and applications*. Cambridge University Press, 2008.
- [31] Xiaoyun Li and Ping Li. Generalization error analysis of quantized compressive learning. In *Advances in Neural Information Processing Systems (NeurIPS)*, Vancouver, Canada, 2019.
- [32] Stuart P. Lloyd. Least squares quantization in PCM. *IEEE Trans. Information Theory*, 28(2):129–136, 1982.
- [33] Joel Max. Quantizing for minimum distortion. *IRE Trans. Information Theory*, 6(1):7–12, 1960.
- [34] S Sandeep Pradhan and Kannan Ramchandran. Group-theoretic construction and analysis of generalized coset codes for symmetric/asymmetric distributed source coding. In *Proceedings of Conference on Information Sciences and Systems (CISS)*, 2000.
- [35] Santosh S. Vempala. *The Random Projection Method*. American Mathematical Society, 2004.
- [36] Ossama Younis and Sonia Fahmy. Distributed clustering in ad-hoc sensor networks: A hybrid, energy-efficient approach. In *Proceedings the 23rd Annual Joint Conference of the IEEE Computer and Communications Societies (INFOCOM)*, Hong Kong, China, 2004.
- [37] Argyrios Zymnis, Stephen P. Boyd, and Emmanuel J. Candès. Compressed sensing with quantized measurements. *IEEE Signal Process. Lett.*, 17(2):149–152, 2010.